shown that *miR-122* is significantly downregulated in HCC with intrahepatic metastasis and negatively regulates tumorigenesis, and that one of its targets, ADAM17, is involved in metastasis. Silencing of ADAM17 resulted in a dramatic reduction of *in vitro* migration, invasion, *in vivo* tumorigenesis, angiogenesis and local invasion in the livers of nude mice. Thus, *miR-122* plays a role in the intrahepatic metastases of metastasized HCC by suppressing angiogenesis via regulation of ADAM17.[61] Together these results indicate that *miR-122* is inactivated in HCC and has multiple functions as a tumor suppressor miRNA during hepatocarcinogenesis. *miR-122* is a promising target for HCC treatment as well as a diagnostic and prognostic marker for the progression of HCC.

The *let-7* family plays a critical role in tumorigenesis by functioning as potential tumor suppressors. The expression of *let-7g* has been shown to be markedly decreased in HCC cells, and proliferation of HCC cells was significantly inhibited after the transfection of *let-7g*, indicating that *let-7g* may act as a tumor suppressor gene that inhibits HCC cell proliferation by downregulating c-Myc.[62] The expression level of *let-7g* was also decreased in metastatic HCC compared to metastasis-free HCC. The low expression level of *let-7g* in tumor tissue was predictive of poor survival in HCC patients. Type I collagen-α2 (COL1A2) and Bcl-xL, an anti-apoptotic member of the Bcl-2 family, were validated as direct targets of *let-7g*. *let-7g* may suppress HCC metastasis and induce apoptosis in HCC cells through targeting COL1A2 and Bcl-xL, respectively.[63,64]

Expression level of *miR-101* was significantly decreased in HCC cell lines and HCC tissues compared with their non-tumor counterparts. Ectopic expression of *miR-101* dramatically suppressed the ability of HCC cells to form colonies *in vitro* and to develop tumors in nude mice. *miR-101* repressed Mcl-1 expression as its target oncogene. These results indicate that *miR-101* may exert its pro-apoptotic function via targeting Mcl-1.[65] Li and associates reported that *miR-101* was significantly downregulated in HCC tissues compared with matching non-tumor liver tissues. They also showed that *miR-101* repressed the expression of *v-fos* FBJ murine osteosarcoma viral oncogene homolog (FOS) oncogene, a key component of activator protein-1 (AP-1) transcription factor. In *in vitro* invasion and migration assays, enhanced *miR-101* expression inhibited the invasion and migration of cultured HCC cells, suggesting that *miR-101* plays an important role as a tumor suppressor by suppressing the FOS oncogene in HCC cells.[66]

On the other hand, *miR-221* and *miR-222* have been reported to be overexpressed in HCC as well as in other malignancies and regulate p27 as their target.[67] Fornari and colleagues reported that the cyclin-dependent kinase inhibitor p57 is also a direct target of *miR-221*. Downregulation of both p27 and p57 occurred in response to *miR-221* transfection into HCC-derived cells, and significant upregulation of both p27 and p57 occurred in response to anti-*miR-221* transfection. The results suggest that *miR-221* has an oncogenic function in hepatocarcinogenesis by targeting p27 and p57, hence promoting proliferation by controlling cell-cycle inhibitors.[68] *miR-221* also targets Bmf, a pro-apoptotic BH3-only protein, and inhibits apoptosis of cells. *MiR-221* overexpression is associated with a more aggressive phenotype of HCC.[69] In addition, DNA damage-inducible transcript 4 (DDIT4), a modulator of the mammalian target of rapamycin pathway, was identified as a target of *miR-221*, indicating an important contribution for *miR-221* in hepatocarcinogenesis.[70] Garofalo and coworkers reported that *miR-221* and *miR-222* are overexpressed in HCC cells, as compared with normal liver cells. They also show that *miR-221* and *miR-222* induce tumor necrosis factor-related apoptosis-inducing ligand resistance and enhance cellular migration through the activation of the Akt pathway and metallopeptidases by targeting phosphatase and tensin homolog and tissue inhibitor of matrix metalloproteinase 3 tumor suppressors and that the MET oncogene is involved in *miR-221* and *miR-222* activation through c-Jun transcription factor.[71] These studies strongly suggest that *miR-221* and *miR-222* are oncogenic miRNA that play critical roles in the initiation and progression of HCC.

EPIGENETIC SILENCING OF TUMOR SUPPRESSOR MIRNA IN HCC

BECAUSE MIRNA HAVE large-scale effects through regulation of a variety of target genes during carcinogenesis, understanding the regulatory mechanisms controlling miRNA expression is important. Many miRNA are expressed in a tissue- and tumor-specific manner, implying that some miRNA are subject to epigenetic control. We have shown that approximately 5% of human miRNA are upregulated more than threefold by treatment of T24 bladder cancer cells with the DNA demethylating agent 5-Aza-CdR and the HDAC inhibitor 4-phenylbutyric acid (PBA). In particular, *miR-127*, which is embedded in a CpG island, is remarkably induced by a decrease in DNA methylation levels and an

increase in active histone marks around the promoter region of the *miR-127* gene. In addition, activation of *miR-127* by epigenetic treatment induced downregulation of its target oncogene *BCL6*.[32] We have also demonstrated that treatment of gastric cancer cells with 5-Aza-CdR and PBA induces activation of *miR-512-5p* which is located at Alu repeats on chromosome 19. Activation of *miR-512-5p* by epigenetic treatment induces suppression of *MCL1*, resulting in apoptosis of gastric cancer cells.[72] These results indicate that chromatin remodeling by epigenetic treatment can directly activate miRNA expression and that activation of silenced tumor suppressor miRNA could be a novel therapeutic approach for human cancers.

Lujambio *et al.*[73] compared miRNA expression profiling between the wild-type HCT116 colon cancer cell line and HCT116 after genetic disruption of both *DNMT1* and *DNMT3b* (DKO cells). They found that 18 out of 320 miRNA are significantly upregulated in DKO cells. In particular, *miR-124* is silenced by its own CpG island hypermethylation in human tumors, but can be activated by inhibition of DNA methylation. They also demonstrated that the oncogene cyclin-dependent kinase 6 (CDK6) is a target of *miR-124* and that epigenetic silencing of *miR-124* in cancer cells modulates *CDK6* activity. Furuta and associates have also demonstrated that *miR-124* and *miR-203* are silenced by CpG island methylation in primary tumors of HCC. In addition, ectopic expression of *miR-124* or *miR-203* in HCC cells lacking their expression inhibited cell growth by suppression of their possible targets, CDK6, vimentin (VIM), SET and MYND domain containing 3 (SMYD3) and IQ motif containing GTPase activating protein 1 or adenosine triphosphate-binding cassette, subfamily E, member 1, respectively.[74] *miR-1* expression is markedly reduced by aberrant CpG island methylation in HCC compared with matching liver tissues. Reactivation of *miR-1 by* the DNA methylation inhibitor 5-azacytidine with downregulation of its target genes *FoxP1*, *MET* and *HDAC4* suppresses proliferation of HCC cells.[75] As summarized in Table 1, several specific miRNA have been reported to be directly regulated from their own promoters by epigenetic alterations in HCC.[76,77] These findings indicate that specific miRNA including *miR-1*, *miR-124* and *miR-203* are tumor-suppressor miRNA that inhibit their target oncogenes and are epigenetically silenced during hepatocarcinogenesis. Reactivation of these miRNA by chromatin-modifying drugs such as DNA methylation inhibitor and HDAC inhibitor may be a novel therapeutic strategy for HCC.

Table 1 miRNA inactivated by DNA hypermethylation in hepatocellular carcinoma

miRNA	Target genes	References
miR-1	*FoxP1, MET, HDAC4*	65
miR-124	*CDK6, VIM, SMYD3, IQGAP1*	64
miR-125b	*PIGF*	66
miR-203	*ABCE1*	64
miR-520e	*NIK*	67

CHROMATIN-MODIFYING FACTORS REGULATED BY MIRNA

RECENT STUDIES HAVE reported that some miRNA can regulate the key chromatin-modifying factors for DNA methylation and histone modifications such as *DNMT1*, *DNMT3A*, *DNMT3B* and *EZH2* as their targets, suggesting that these miRNA have important roles in the epigenetic control of gene expression (Table 2).[78]

It has been shown that *miR-152* is downregulated in HCC and targets *DNMT1*.[79] *miR-152* may act as a tumor suppressor via suppression of *DNMT1* and it can be a new target for epigenetic therapy of HCC. PRC1 and PRC2-mediated epigenetic regulation is critical for

Table 2 Chromatin modifying factors regulated by miRNA

Chromatin modifying factors	miRNA	Expression	References
DNMT1	*miR-152*	*miR-152* is silenced in HCC with upregulation of *DNMT1*	69
DNMT3A, DNMT3B	*miR-29a, -29b, -29c*	*miR-29* family are silenced in lung cancer with upregulation of *DNMT3A* and *DNMT3B*	68
EZH2	*miR-101*	*miR-101* is silenced in cancer with upregulation of *EZH2*	70,71

maintaining cellular homeostasis. PRC2 mediates epigenetic gene silencing by tri-methylating histone H3 lysine 27 (H3K27me3) and is known to aberrantly silence tumor suppressor genes in cancer. *EZH2*, the catalytic subunit of PRC2, enhances tumorigenesis and is commonly overexpressed in several types of cancer. *miR-101* is downregulated in bladder cancer, and *miR-101* directly represses *EZH2*. This suggests that abnormal downregulation of *miR-101* could lead to the overexpression of *EZH2* frequently seen in cancer. *miR-101* may be a potent tumor suppressor by altering global chromatin structure through repression of *EZH2*.[80,81]

The CCCTC-binding factor, CTCF, is known to bind insulators and exhibits an enhancer-blocking and barrier function, and more recently, it also contributes to the 3-D organization of the genome. CTCF can also serve as a barrier against the spread of DNA methylation and histone repressive marks over promoter regions of tumor suppressor genes. Recent studies have shown that CTCF is also involved in the regulation of miRNA in cancer cells and stem cells.[82] Watanabe *et al.*[83] have reported that CTCF plays important roles in the regulation of the cytokine genes *TNF* and *LT* in HCC cells.

Figure 3 shows a model summarizing the cross-talk between epigenetics and miRNA and the link between miRNA and regulated genes. In normal hepatocytes, *miR-152* is substantially expressed, and its target gene *DNMT1* is suppressed. On the other hand, *miR-152* is downregulated in HCC cells, resulting in overexpression of *DNMT1* accompanied by aberrant DNA methylation of some tumor suppressor miRNA such as *miR-1* and *miR-124*. Downregulation of *miR-1* and *miR-124* cause activation of their target oncogenes. Thus, epigenetics and miRNA are affected by each other and their cross-talk may play critical roles in the hepatocarcinogenesis.

PERSPECTIVES

AS DESCRIBED ABOVE, it is increasingly apparent that cross-talk between epigenetics and miRNA is quite important in the molecular pathogenesis of HCC. A promising option for cancer treatment is the use of epigenetic drugs which inhibit tumor growth by several mechanisms including restoring the expression of epigenetically silenced tumor suppressor genes and miRNA.[84] We recently found that a HDAC inhibitor, suberoylanilide hydroxamic acid, suppressed hepatitis C virus RNA replication via the epigenetic mechanism in a replicon cells[85] in addition to induction of apoptosis in liver cancer cells through enhanced expression of several specific miRNA (paper in preparation). These findings suggested that an epigenetic approach could potentially

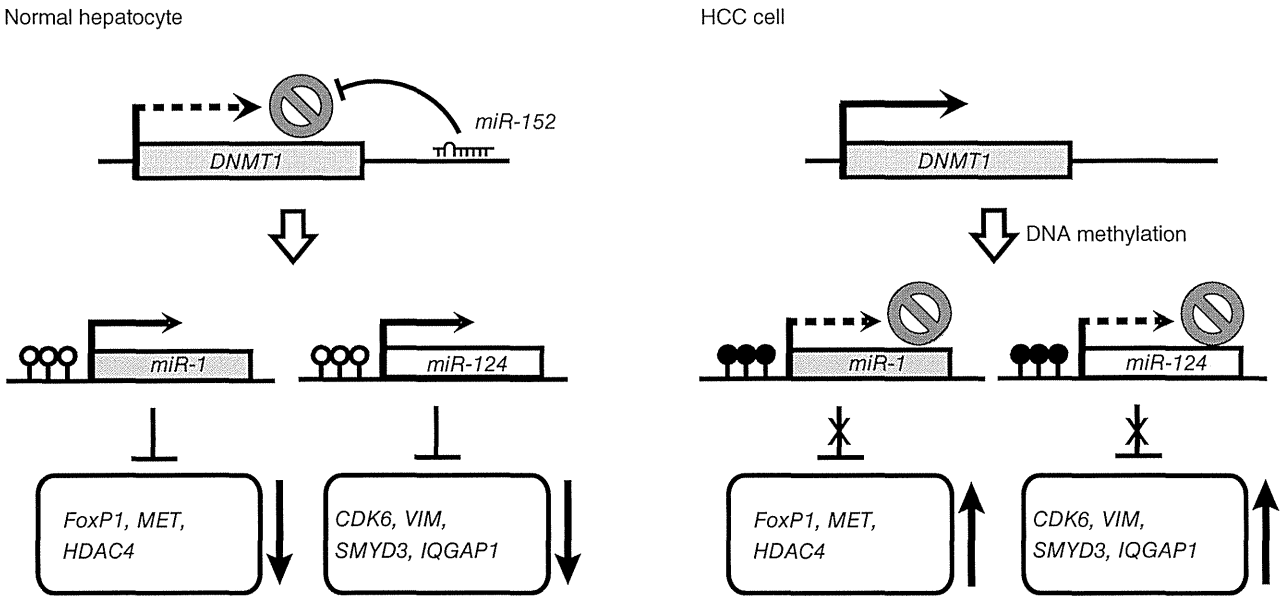

Figure 3 A model summarizing the cross-talk between epigenetics and miRNA. In normal hepatocytes, *miR-152* is substantially expressed, and its target gene *DNMT1* is suppressed. On the other hand, *miR-152* is downregulated in hepatocellular carcinoma (HCC) cells, resulting in overexpression of *DNMT1* accompanied by aberrant DNA methylation of some tumor suppressor miRNA such as *miR-1* and *miR-124*. Downregulation of *miR-1* and *miR-124* causes activation of their target oncogenes.

play not only anticancer but also antiviral roles in HCC treatment. Moreover, inhibitors of DNA methylation and histone deacetylation can work synergistically to suppress growth of cancer cell lines both *in vitro* and *in vivo*. Many epigenetic drugs have shown promising results in clinical trials and recent advances in research suggest a new anticancer effect of this class of drugs. However, these drugs have some problems to be resolved such as specificity of DNA methylation inhibition. Current drugs for inhibitors of DNA methylation and HDAC cannot target specific genes and miRNA and may activate some oncogenes and oncogenic miRNA. Further studies are necessary to develop promising drugs which can target specific genes and miRNA with minimal side-effects. By inducing expression of tumor suppressor genes and miRNA, epigenetic treatment not only inhibits the growth of HCC, but may also inhibit the invasiveness and metastatic potential of HCC.

ACKNOWLEDGMENTS

THIS WORK WAS supported by a Grant-in-Aid for Young Scientists A (23680090 to Y. S.) and a Grant-in-Aid for Scientific Research C (24590993 to H. S.) from the Japan Society for the Promotion of Science (JSPS), Takeda Science Foundation (to Y. S.) and Inaida Foundation (to H. S.).

REFERENCES

1 Farazi PA, DePinho RA. The genetic and environmental basis of hepatocellular carcinoma. *Discov Med* 2006; 6: 182–6.
2 Farazi PA, DePinho RA. Hepatocellular carcinoma pathogenesis: from genes to environment. *Nat Rev Cancer* 2006; 6: 674–87.
3 Gal-Yam EN, Saito Y, Egger G, Jones PA. Cancer epigenetics: modifications, screening, and therapy. *Annu Rev Med* 2008; 59: 267–80.
4 Yoo CB, Jones PA. Epigenetic therapy of cancer: past, present and future. *Nat Rev Drug Discov* 2006; 5: 37–50.
5 Riggs MG, Whittaker RG, Neumann JR, Ingram VM. n-Butyrate causes histone modification in HeLa and Friend erythroleukaemia cells. *Nature* 1977; 268: 462–4.
6 Boffa LC, Vidali G, Mann RS, Allfrey VG. Suppression of histone deacetylation in vivo and in vitro by sodium butyrate. *J Biol Chem* 1978; 253: 3364–6.
7 Morrison DJ, Mackay WG, Edwards CA, Preston T, Dodson B, Weaver LT. Butyrate production from oligofructose fermentation by the human faecal flora: what is the contribution of extracellular acetate and lactate? *Br J Nutr* 2006; 96: 570–7.
8 Morita A, Tsao D, Kim YS. Effect of sodium butyrate on alkaline phosphatase in HRT-18, a human rectal cancer cell line. *Cancer Res* 1982; 42: 4540–5.
9 Augeron C, Laboisse CL. Emergence of permanently differentiated cell clones in a human colonic cancer cell line in culture after treatment with sodium butyrate. *Cancer Res* 1984; 44: 3961–9.
10 Gahmberg CG, Nilsson K, Andersson LC. Specific changes in the surface glycoprotein pattern of human promyelocytic leukemic cell line HL-60 during morphologic and functional differentiation. *Proc Natl Acad Sci U S A* 1979; 76: 4087–91.
11 Warrell RP, Jr, He LZ, Richon V, Calleja E, Pandolfi PP. Therapeutic targeting of transcription in acute promyelocytic leukemia by use of an inhibitor of histone deacetylase. *J Natl Cancer Inst* 1998; 90: 1621–5.
12 Saito H, Morizane T, Watanabe T *et al.* Differentiating effect of sodium butyrate on human hepatoma cell lines PLC/PRF/5, HCC-M and HCC-T. *Int J Cancer* 1991; 48: 291–6.
13 Tsukamoto H, Zhu NL, Asahina K, Mann DA, Mann J. Epigenetic cell fate regulation of hepatic stellate cells. *Hepatol Res* 2011; 41: 675–82.
14 Kondo Y, Shen L, Suzuki S *et al.* Alterations of DNA methylation and histone modifications contribute to gene silencing in hepatocellular carcinomas. *Hepatol Res* 2007; 37: 974–83.
15 Wang L, Wang WL, Zhang Y, Guo SP, Zhang J, Li QL. Epigenetic and genetic alterations of PTEN in hepatocellular carcinoma. *Hepatol Res* 2007; 37: 389–96.
16 Zhang J, Gong C, Bing Y, Li T, Liu Z, Liu Q. Hypermethylation-repressed methionine adenosyltransferase 1A as a potential biomarker for hepatocellular carcinoma. *Hepatol Res* 2013; 43: 374–83.
17 Saito H, Kagawa T, Tada S *et al.* Effect of dexamethasone, dimethylsulfoxide and sodium butyrate on a human hepatoma cell line PLC/PRF/5. *Cancer Biochem Biophys* 1992; 13: 75–84.
18 Saito H, Tada S, Ebinuma H *et al.* Changes of antigen expression on human hepatoma cell lines caused by sodium butyrate, a differentiation inducer. *J Gastroenterol* 1994; 29: 733–9.
19 Tada S, Saito H, Ebinuma H *et al.* Reduction of LAK-sensitivity and changes in antigen expression on hepatoma cells by sodium butyrate. *Cancer Biochem Biophys* 1996; 15: 177–86.
20 Wakabayashi K, Saito H, Ebinuma H *et al.* Bcl-2 related proteins are dramatically induced at the early stage of differentiation in human liver cancer cells by a histone deacetylase inhibitor projecting an anti-apoptotic role during this period. *Oncol Rep* 2000; 7: 285–8.
21 Saito H, Ebinuma H, Takahashi M *et al.* Loss of butyrate-induced apoptosis in human hepatoma cell lines HCC-M and HCC-T having substantial Bcl-2 expression. *Hepatology* 1998; 27: 1233–40.

22 Ebinuma H, Saito H, Saito Y *et al.* Antisense oligodeoxynucleotide against c-myc mRNA induces differentiation of human hepatocellular carcinoma cells. *Int J Oncol* 1999; 15: 991–9.
23 Ebinuma H, Saito H, Kosuga M *et al.* Reduction of c-myc expression by an antisense approach under Cre/loxP switching induces apoptosis in human liver cancer cells. *J Cell Physiol* 2001; 188: 56–66.
24 Masuda T, Saito H, Kaneko F *et al.* Up-regulation of E-cadherin and I-catenin in human hepatocellular carcinoma cell lines by sodium butyrate and interferon-alpha. *In Vitro Cell Dev Biol Anim* 2000; 36: 387–94.
25 Kaneko F, Saito H, Saito Y *et al.* Down-regulation of matrix-invasive potential of human liver cancer cells by type I interferon and a histone deacetylase inhibitor sodium butyrate. *Int J Oncol* 2004; 24: 837–45.
26 Nakamura M, Saito H, Ebinuma H *et al.* Reduction of telomerase activity in human liver cancer cells by a histone deacetylase inhibitor. *J Cell Physiol* 2001; 187: 392–401.
27 Wakabayashi K, Saito H, Kaneko F, Nakamoto N, Tada S, Hibi T. Gene expression associated with the decrease in malignant phenotype of human liver cancer cells following stimulation with a histone deacetylase inhibitor. *Int J Oncol* 2005; 26: 233–9.
28 Yasuda E, Kumada T, Toyoda H *et al.* Evaluation for clinical utility of GPC3, measured by a commercially available ELISA kit with Glypican-3 (GPC3) antibody, as a serological and histological marker for hepatocellular carcinoma. *Hepatol Res* 2010; 40: 477–85.
29 Suzuki E, Chiba T, Zen Y *et al.* Aldehyde dehydrogenase 1 is associated with recurrence-free survival but not stem cell-like properties in hepatocellular carcinoma. *Hepatol Res* 2012; 42: 1100–11.
30 Moribata K, Tamai H, Shingaki N *et al.* Assessment of malignant potential of small hypervascular hepatocellular carcinoma using B-mode ultrasonography. *Hepatol Res* 2011; 41: 233–9.
31 Ijichi H, Shirabe K, Taketomi A *et al.* Clinical usefulness of (18) F-fluorodeoxyglucose positron emission tomography/computed tomography for patients with primary liver cancer with special reference to rare histological types, hepatocellular carcinoma with sarcomatous change and combined hepatocellular and cholangiocarcinoma. *Hepatol Res* 2013; 43: 481–7.
32 Saito Y, Liang G, Egger G *et al.* Specific activation of microRNA-127 with downregulation of the proto-oncogene BCL6 by chromatin-modifying drugs in human cancer cells. *Cancer Cell* 2006; 9: 435–43.
33 Kim N, Kim H, Jung I, Kim Y, Kim D, Han YM. Expression profiles of miRNAs in human embryonic stem cells during hepatocyte differentiation. *Hepatol Res* 2011; 41: 170–83.
34 Liu D, Fan J, Zeng W, Zhou Y, Ingvarsson S, Chen H. Quantitative analysis of miRNA expression in several developmental stages of human livers. *Hepatol Res* 2010; 40: 813–22.
35 Lu J, Getz G, Miska EA *et al.* MicroRNA expression profiles classify human cancers. *Nature* 2005; 435: 834–8.
36 Calin GA, Croce CM. MicroRNA signatures in human cancers. *Nat Rev Cancer* 2006; 6: 857–66.
37 Huang XH, Wang Q, Chen JS *et al.* Bead-based microarray analysis of microRNA expression in hepatocellular carcinoma: miR-338 is downregulated. *Hepatol Res* 2009; 39: 786–94.
38 Egger G, Liang G, Aparicio A, Jones PA. Epigenetics in human disease and prospects for epigenetic therapy. *Nature* 2004; 429: 457–63.
39 Okano M, Xie S, Li E. Cloning and characterization of a family of novel mammalian DNA (cytosine-5) methyltransferases. *Nat Genet* 1998; 19: 219–20.
40 Eden A, Gaudet F, Waghmare A, Jaenisch R. Chromosomal instability and tumors promoted by DNA hypomethylation. *Science* 2003; 300: 455.
41 Saito Y, Kanai Y, Sakamoto M, Saito H, Ishii H, Hirohashi S. Expression of mRNA for DNA methyltransferases and methyl-CpG-binding proteins and DNA methylation status on CpG islands and pericentromeric satellite regions during human hepatocarcinogenesis. *Hepatology* 2001; 33: 561–8.
42 Saito Y, Kanai Y, Nakagawa T *et al.* Increased protein expression of DNA methyltransferase (DNMT) 1 is significantly correlated with the malignant potential and poor prognosis of human hepatocellular carcinomas. *Int J Cancer* 2003; 105: 527–32.
43 Okano M, Bell DW, Haber DA, Li E. DNA methyltransferases Dnmt3a and Dnmt3b are essential for de novo methylation and mammalian development. *Cell* 1999; 99: 247–57.
44 Saito Y, Kanai Y, Sakamoto M, Saito H, Ishii H, Hirohashi S. Overexpression of a splice variant of DNA methyltransferase 3b, DNMT3b4, associated with DNA hypomethylation on pericentromeric satellite regions during human hepatocarcinogenesis. *Proc Natl Acad Sci U S A* 2002; 99: 10060–5.
45 Liang G, Lin JC, Wei V *et al.* Distinct localization of histone H3 acetylation and H3-K4 methylation to the transcription start sites in the human genome. *Proc Natl Acad Sci U S A* 2004; 101: 7357–62.
46 Kouzarides T. Chromatin modifications and their function. *Cell* 2007; 128: 693–705.
47 Jenuwein T, Allis CD. Translating the histone code. *Science* 2001; 293: 1074–80.
48 Kondo Y, Shen L, Cheng AS *et al.* Gene silencing in cancer by histone H3 lysine 27 trimethylation independent of promoter DNA methylation. *Nat Genet* 2008; 40: 741–50.
49 Cai MY, Hou JH, Rao HL *et al.* High expression of H3K27me3 in human hepatocellular carcinomas correlates closely with vascular invasion and predicts worse prognosis in patients. *Mol Med* 2011; 17: 12–20.
50 Sudo T, Utsunomiya T, Mimori K *et al.* Clinicopathological significance of EZH2 mRNA expression in patients with

hepatocellular carcinoma. *Br J Cancer* 2005; **92**: 1754–8.
51 Yao JY, Zhang L, Zhang X *et al.* H3K27 trimethylation is an early epigenetic event of p16INK4a silencing for regaining tumorigenesis in fusion reprogrammed hepatoma cells. *J Biol Chem* 2010; **285**: 18828–37.
52 Wu LM, Yang Z, Zhou L *et al.* Identification of histone deacetylase 3 as a biomarker for tumor recurrence following liver transplantation in HBV-associated hepatocellular carcinoma. *PLoS ONE* 2010; **5**: e14460.
53 He L, Hannon GJ. MicroRNAs: small RNAs with a big role in gene regulation. *Nat Rev Genet* 2004; **5**: 522–31.
54 Calin GA, Croce CM. Chromosomal rearrangements and microRNAs: a new cancer link with clinical implications. *J Clin Invest* 2007; **117**: 2059–66.
55 Saito Y, Suzuki H, Hibi T. The role of microRNAs in gastrointestinal cancers. *J Gastroenterol* 2009; **44** (Suppl 19): 18–22.
56 Jopling CL, Yi M, Lancaster AM, Lemon SM, Sarnow P. Modulation of hepatitis C virus RNA abundance by a liver-specific MicroRNA. *Science* 2005; **309**: 1577–81.
57 Fornari F, Gramantieri L, Giovannini C *et al.* MiR-122/cyclin G1 interaction modulates p53 activity and affects doxorubicin sensitivity of human hepatocarcinoma cells. *Cancer Res* 2009; **69**: 5761–7.
58 Lin CJ, Gong HY, Tseng HC, Wang WL, Wu JL. miR-122 targets an anti-apoptotic gene, Bcl-w, in human hepatocellular carcinoma cell lines. *Biochem Biophys Res Commun* 2008; **375**: 315–20.
59 Ma L, Liu J, Shen J *et al.* Expression of miR-122 mediated by adenoviral vector induces apoptosis and cell cycle arrest of cancer cells. *Cancer Biol Ther* 2010; **9**: 554–61.
60 Bai S, Nasser MW, Wang B *et al.* MicroRNA-122 inhibits tumorigenic properties of hepatocellular carcinoma cells and sensitizes these cells to sorafenib. *J Biol Chem* 2009; **284**: 32015–27.
61 Tsai WC, Hsu PW, Lai TC *et al.* MicroRNA-122, a tumor suppressor microRNA that regulates intrahepatic metastasis of hepatocellular carcinoma. *Hepatology* 2009; **49**: 1571–82.
62 Lan FF, Wang H, Chen YC *et al.* Hsa-let-7g inhibits proliferation of hepatocellular carcinoma cells by downregulation of c-Myc and upregulation of p16(INK4A). *Int J Cancer* 2011; **128**: 319–31.
63 Ji J, Zhao L, Budhu A *et al.* Let-7g targets collagen type I alpha2 and inhibits cell migration in hepatocellular carcinoma. *J Hepatol* 2010; **52**: 690–7.
64 Shimizu S, Takehara T, Hikita H *et al.* The let-7 family of microRNAs inhibits Bcl-xL expression and potentiates sorafenib-induced apoptosis in human hepatocellular carcinoma. *J Hepatol* 2010; **52**: 698–704.
65 Su H, Yang JR, Xu T *et al.* MicroRNA-101, down-regulated in hepatocellular carcinoma, promotes apoptosis and suppresses tumorigenicity. *Cancer Res* 2009; **69**: 1135–42.
66 Li S, Fu H, Wang Y *et al.* MicroRNA-101 regulates expression of the v-fos FBJ murine osteosarcoma viral oncogene homolog (FOS) oncogene in human hepatocellular carcinoma. *Hepatology* 2009; **49**: 1194–202.
67 Dai R, Li J, Liu Y *et al.* miR-221/222 suppression protects against endoplasmic reticulum stress-induced apoptosis via p27(Kip1)- and MEK/ERK-mediated cell cycle regulation. *Biol Chem* 2010; **391**: 791–801.
68 Fornari F, Gramantieri L, Ferracin M *et al.* MiR-221 controls CDKN1C/p57 and CDKN1B/p27 expression in human hepatocellular carcinoma. *Oncogene* 2008; **27**: 5651–61.
69 Gramantieri L, Fornari F, Ferracin M *et al.* MicroRNA-221 targets Bmf in hepatocellular carcinoma and correlates with tumor multifocality. *Clin Cancer Res* 2009; **15**: 5073–81.
70 Pineau P, Volinia S, McJunkin K *et al.* miR-221 overexpression contributes to liver tumorigenesis. *Proc Natl Acad Sci U S A* 2010; **107**: 264–9.
71 Garofalo M, Di Leva G, Romano G *et al.* miR-221&222 regulate TRAIL resistance and enhance tumorigenicity through PTEN and TIMP3 downregulation. *Cancer Cell* 2009; **16**: 498–509.
72 Saito Y, Suzuki H, Tsugawa H *et al.* Chromatin remodeling at Alu repeats by epigenetic treatment activates silenced microRNA-512-5p with downregulation of Mcl-1 in human gastric cancer cells. *Oncogene* 2009; **28**: 2738–44.
73 Lujambio A, Ropero S, Ballestar E *et al.* Genetic unmasking of an epigenetically silenced microRNA in human cancer cells. *Cancer Res* 2007; **67**: 1424–9.
74 Furuta M, Kozaki KI, Tanaka S, Arii S, Imoto I, Inazawa J. miR-124 and miR-203 are epigenetically silenced tumor-suppressive microRNAs in hepatocellular carcinoma. *Carcinogenesis* 2010; **31**: 766–76.
75 Datta J, Kutay H, Nasser MW *et al.* Methylation mediated silencing of MicroRNA-1 gene and its role in hepatocellular carcinogenesis. *Cancer Res* 2008; **68**: 5049–58.
76 Alpini G, Glaser SS, Zhang JP *et al.* Regulation of placenta growth factor by microRNA-125b in hepatocellular cancer. *J Hepatol* 2011; **55**: 1339–45.
77 Zhang S, Shan C, Kong G, Du Y, Ye L, Zhang X. MicroRNA-520e suppresses growth of hepatoma cells by targeting the NF-kappaB-inducing kinase (NIK). *Oncogene* 2012; **31**: 3607–20.
78 Fabbri M, Garzon R, Cimmino A *et al.* MicroRNA-29 family reverts aberrant methylation in lung cancer by targeting DNA methyltransferases 3A and 3B. *Proc Natl Acad Sci U S A* 2007; **104**: 15805–10.
79 Huang J, Wang Y, Guo Y, Sun S. Down-regulated microRNA-152 induces aberrant DNA methylation in hepatitis B virus-related hepatocellular carcinoma by targeting DNA methyltransferase 1. *Hepatology* 2010; **52**: 60–70.
80 Friedman JM, Liang G, Liu CC *et al.* The putative tumor suppressor microRNA-101 modulates the cancer epige-

nome by repressing the polycomb group protein EZH2. *Cancer Res* 2009; 69: 2623–9.
81 Varambally S, Cao Q, Mani RS *et al.* Genomic loss of microRNA-101 leads to overexpression of histone methyltransferase EZH2 in cancer. *Science* 2008; 322: 1695–9.
82 Saito Y, Saito H. Role of CTCF in the regulation of microRNA expression. *Front Genet* 2012; 3: 186.
83 Watanabe T, Ishihara K, Hirosue A *et al.* Higher-order chromatin regulation and differential gene expression in the human tumor necrosis factor/lymphotoxin locus in hepatocellular carcinoma cells. *Mol Cell Biol* 2012; 32: 1529–41.
84 Jones PA, Baylin SB. The epigenomics of cancer. *Cell* 2007; 128: 683–92.
85 Sato A, Saito Y, Sugiyama K *et al.* Suppressive effect of the histone deacetylase inhibitor, suberoylanilide hydroxamic acid (SAHA), on hepatitis C virus replication via epigenetic changes in host cells. *J Cell Biochem* 2013 (in press).

HEPATOLOGY
Official Journal of the American Association for the Study of Liver Diseases

Free Cholesterol Accumulation in Hepatic Stellate Cells: Mechanism of Liver Fibrosis Aggravation in Nonalcoholic Steatohepatitis in Mice

Kengo Tomita,[1,2]* Toshiaki Teratani,[2]* Takahiro Suzuki,[2] Motonori Shimizu,[1] Hirokazu Sato,[1] Kazuyuki Narimatsu,[1] Yoshikiyo Okada,[1] Chie Kurihara,[1] Rie Irie,[3] Hirokazu Yokoyama,[4] Katsuyoshi Shimamura,[2] Shingo Usui,[1,2] Hirotoshi Ebinuma,[2] Hidetsugu Saito,[5] Chikako Watanabe,[1] Shunsuke Komoto,[1] Atsushi Kawaguchi,[1] Shigeaki Nagao,[1] Kazuo Sugiyama,[2] Ryota Hokari,[1] Takanori Kanai,[2] Soichiro Miura,[1] and Toshifumi Hibi[2]

Although nonalcoholic steatohepatitis (NASH) is associated with hypercholesterolemia, the underlying mechanisms of this association have not been clarified. We aimed to elucidate the precise role of cholesterol in the pathophysiology of NASH. C57BL/6 mice were fed a control, high-cholesterol (HC), methionine-choline-deficient (MCD), or MCD+HC diet for 12 weeks or a control, HC, high-fat (HF), or HF+HC diet for 24 weeks. Increased cholesterol intake accelerated liver fibrosis in both the mouse models without affecting the degree of hepatocellular injury or Kupffer cell activation. The major causes of the accelerated liver fibrosis involved free cholesterol (FC) accumulation in hepatic stellate cells (HSCs), which increased Toll-like receptor 4 protein (TLR4) levels through suppression of the endosomal-lysosomal degradation pathway of TLR4, and thereby sensitized the cells to transforming growth factor (TGF)β-induced activation by down-regulating the expression of bone morphogenetic protein and activin membrane-bound inhibitor. Mammalian-cell cholesterol levels are regulated by way of a feedback mechanism mediated by sterol regulatory element-binding protein 2 (SREBP2), maintaining cellular cholesterol homeostasis. Nevertheless, HSCs were sensitive to FC accumulation because the high intracellular expression ratio of SREBP cleavage-activating protein (Scap) to insulin-induced gene (Insig) disrupted the SREBP2-mediated feedback regulation of cholesterol homeostasis in these cells. HSC activation subsequently enhanced the disruption of the feedback system by Insig-1 down-regulation. In addition, the suppression of peroxisome proliferator-activated receptor γ signaling accompanying HSC activation enhanced both SREBP2 and microRNA-33a signaling. Consequently, FC accumulation in HSCs increased and further sensitized these cells to TGFβ-induced activation in a vicious cycle, leading to exaggerated liver fibrosis in NASH. *Conclusion*: These characteristic mechanisms of FC accumulation in HSCs are potential targets to treat liver fibrosis in liver diseases including NASH. (HEPATOLOGY 2014;59:154-169)

Abbreviations: ABCA1, adenosine triphosphate-binding cassette A1; ALT, alanine aminotransferase; Bambi, bone morphogenetic protein and activin membrane-bound inhibitor; CCl_4, carbon tetrachloride; CE, cholesterol ester; COPII, coat protein complex II; ER, endoplasmic reticulum; FBS, fetal bovine serum; FC, free cholesterol; HC, high cholesterol; HF, high fat; HMGCR, 3-hydroxy-3-methyl-glutaryl-CoA reductase; HSC, hepatic stellate cell; ICAM-1, intercellular adhesion molecule-1; Insig, insulin-induced gene; LDLR, low-density lipoprotein receptor; LPS, lipopolysaccharide; MβCD, methyl-β-cyclodextrin; MCD, methionine-choline deficient; mRNA, messenger RNA; NASH, nonalcoholic steatohepatitis; NPC1, Niemann-Pick C1; PCR, polymerase chain reaction; PPAR, peroxisome proliferator-activated receptor; Scap, SREBP cleavage-activating protein; siRNA, small interfering RNA; SMA, smooth muscle actin; SREBP, sterol regulatory element-binding protein; TGF, transforming growth factor; TLR4, Toll-like receptor 4; TNF, tumor necrosis factor; TUNEL, terminal deoxynucleotidyl transferase-mediated deoxyuridine nick-end labeling; VCAM-1, vascular cell adhesion molecule-1.

From the [1]Division of Gastroenterology and Hepatology, Department of Internal Medicine, National Defense Medical College, Saitama, Japan; [2]Division of Gastroenterology and Hepatology, Department of Internal Medicine, Keio University School of Medicine, Tokyo, Japan; [3]Department of Pathology, Kawasaki Municipal Hospital, Kanagawa, Japan; [4]Health Center, Keio University School of Medicine, Tokyo, Japan; [5]Graduate School of Pharmaceutical Sciences, Keio University Faculty of Pharmacy, Tokyo, Japan.

Nonalcoholic steatohepatitis (NASH) is a progressive disease that can cause cirrhosis or liver-related complications.[1] It very often accompanies lifestyle diseases including hypercholesterolemia. Several studies have shown that statins and ezetimibe (cholesterol-lowering agents) improve liver fibrosis in patients with NASH.[2] Furthermore, we have recently reported that free cholesterol (FC) accumulation in hepatic stellate cells (HSCs) plays an important role in the pathogenesis of liver fibrosis.[3] These results drew our attention to the role of cholesterol in the pathogenesis of liver fibrosis in NASH.

Cholesterol homeostasis is tightly regulated by way of a feedback system mediated by sterol regulatory element-binding protein (SREBP)2.[4,5] The low-density lipoprotein receptor (LDLR) and 3-hydroxy-3-methylglutaryl-CoA reductase (HMGCR), which play important roles in maintaining cholesterol uptake and synthesis, respectively, are predominantly regulated by SREBP2.[6] Nascent SREBP2 localizes to the endoplasmic reticulum (ER) membrane and forms tight complexes with SREBP cleavage-activating protein (Scap), a membrane-embedded escort protein.[7] When membrane cholesterol levels are low, the SREBP2-Scap complex is incorporated into the coat protein complex II (COPII)-coated vesicles.[6,8] Consequently, SREBP2 translocates to the nucleus and activates transcription of several target genes involved in the biosynthesis and uptake of cholesterol.[6] When excess cholesterol accumulates in the ER membranes, it changes Scap to an alternate conformation, allowing it to bind to resident ER proteins, insulin-induced gene (Insig)-1, and Insig-2.[9] This binding precludes the binding of COPII. Consequently, the SREBP2-Scap complex remains in the ER, transcription of the target genes declines, and cholesterol synthesis and uptake fall.[4,6]

Furthermore, recent studies have shown that the primary transcript of SREBP2 also encodes miR-33a, a microRNA that regulates cholesterol metabolism by way of factors such as adenosine triphosphate-binding cassette A1 (ABCA1) and Niemann-Pick C1 (NPC1), suggesting transcriptional regulation by *SREBF2* modulates the cellular capacity for producing not only an active transcription factor but also the expression of miR-33a.[10]

By studying two mouse models of NASH, we attempted to clarify the precise role of cholesterol in the pathophysiology of NASH. As we found that the major causes of the exacerbation of liver fibrosis in NASH involved FC accumulation in HSCs, we investigated the underlying mechanisms of FC accumulation in HSCs and its role in the pathogenesis of NASH.

Materials and Methods

Please refer to the Supporting Materials and Methods for more detailed descriptions.

Reagents. Reagents were obtained as follows: low density lipoprotein (LDL), methyl-β-cyclodextrin (MβCD)/cholesterol complex, lipopolysaccharide (LPS), chloroquine, and MG-132 were from Sigma (St. Louis, MO). 25-HC was from Wako Pure Chemical Industries (Osaka, Japan). Transforming growth factor beta (TGFβ) was from R&D Systems (Minneapolis, MN). Peroxisome proliferator-activated receptor gamma (PPARγ)-small interfering RNA (siRNA), SREBP2-siRNA, LDLR-siRNA, Scap-siRNA, Insig-1-siRNA, bone morphogenetic protein and activin membrane-bound inhibitor (Bambi)-siRNA, and control-siRNA were from Invitrogen (Carlsbad, CA). Anti-miR33a, pre-miR33a, and control-miR33a were from Ambion (Austin, TX).

Animal Studies. Nine-week-old male C57BL/6J mice (CLEA Japan, Tokyo, Japan) were fed a CE-2 (control; CLEA Japan), CE-2 with 1% cholesterol (HC), methionine-choline-deficient (MCD; Cat. No. 960439; ICN, Aurora, OH), or MCD with 1% cholesterol (MCD+HC) diet for 12 weeks. As another animal model of NASH, 9-week-old male C57BL/6J mice were also fed a CE-2, HC, high-fat (HF; prepared by CLEA Japan according to the #101447 composition of

Received September 30, 2012; accepted June 20, 2013.

Supported in part by a Grant-in-Aid for Scientific Research from the Ministry of Education, Culture, Sports, Science, and Technology of Japan (to K. Tomita)

**These authors contributed equally to this work.*

Address reprint requests to: Kengo Tomita, M.D., Division of Gastroenterology and Hepatology, Department of Internal Medicine, National Defense Medical College, 3-2 Namiki, Tokorozawa-shi, Saitama 359-8513, Japan. E-mail: kengo@ndmc.ac.jp; fax: +81 4-2996-5201.

View this article online at wileyonlinelibrary.com.

DOI 10.1002/hep.26604

Potential conflict of interest: Nothing to report.

Additional Supporting Information may be found in the online version of this article.

Dyets, Bethlehem, PA), or HF with 1% cholesterol (HF+HC) diet for 24 weeks. In the same way, 7-8-week-old C57BL/6 Toll-like receptor (TLR)4-deficient mice (Oriental BioService, Kyoto, Japan) were fed the control, HC, MCD, or MCD+HC diets for 8 weeks or the control, HC, HF, or HF+HC diets for 20 weeks. All animals received humane care in compliance with the criteria outlined in the "Guide for the Care and Use of Laboratory Animals," prepared by the US National Academy of Sciences and published by the US National Institutes of Health.

HSC Isolation and Cell Culture. Wild-type or TLR4-deficient HSCs were isolated from the livers of mice as described.[3] We cultured HSCs on uncoated 6-well plastic tissue culture dishes in serum-depleted Dulbecco's modified Eagle's medium (DMEM), DMEM containing 1% or 10% fetal bovine serum (FBS), and used them as nonpassaged primary cultures or cultures at passage 3-6.

Statistical Analysis. All data are expressed as means (standard error of the mean [SEM]). Statistical analyses were performed using the unpaired Student *t* test or one-way analysis of variance (ANOVA) ($P < 0.05$ was considered significant). When the ANOVA analyses were applied, differences in mean values among groups were examined by Fisher's multiple comparison test.

Results

Increased Cholesterol Intake Accelerates Liver Fibrosis in NASH Without Affecting the Degree of Hepatocellular Injury or Macrophage Recruitment or Activation. Compared with the livers of the MCD diet-fed mice, the livers of the MCD+HC diet-fed mice showed markedly increased centrizonal fibrosis (Supporting Fig. 1A-C). As observed in the MCD diet-induced NASH model, the extent of fibrosis was significantly enhanced in the livers of the HF+HC diet-fed mice, compared with the HF diet-fed mice (Supporting Fig. 1D-F).

HC diet feeding alone was not sufficient to cause liver fibrosis over 12 and 24 weeks (Supporting Fig. 1). In addition, increased intake of cholesterol did not significantly impact hepatocellular damage in the two mouse models of NASH (Supporting Fig. 2). There was no impact on the hepatic messenger RNA (mRNA) levels of Cyp27a1 or on the hepatic content of mitochondrial FC (Supporting Fig. 3).

Similarly, the increased cholesterol intake did not increase macrophage recruitment or activation in either of the two mouse models of NASH (Supporting Fig. 4). Neither did the increased cholesterol intake induce the formation of hepatic macrophage foam cells or cause liver inflammation in these mouse models (Supporting Figs. 1A,D, 5A). In Kupffer cells, there was also no impact on the mRNA levels of Cyp27a1 or on the cholesterol content of both the mitochondria and late endosomes/lysosomes (Supporting Fig. 5B-D). Furthermore, the increased cholesterol intake significantly exaggerated liver fibrosis in Kupffer cell-depleted mice with NASH (Supporting Fig. 6).

FC Accumulation in HSCs Is Enhanced in NASH and Up-Regulates TLR4 Protein Expression and Down-Regulates Bambi mRNA Expression in HSCs. HC, MCD, and HF diet feeding significantly increased FC levels in HSCs compared with the corresponding control diet feeding (Supporting Fig. 7A,D). Further, FC levels were significantly higher in HSCs from the MCD+HC and HF+HC diet-fed groups than in those from the other corresponding groups (Supporting Fig. 7A,D).

The mRNA expression levels of Bambi, the TGFβ pseudoreceptor, were significantly lower in HSCs from the HC, MCD, and HF diet-fed groups than in those from the corresponding control diet-fed groups and in HSCs from the MCD+HC and HF+HC diet-fed groups than in those from the other corresponding groups (Supporting Fig. 7B,E).

HC, MCD, and HF diet feeding increased the amount of TLR4 protein expressed in HSCs. In addition, HSCs from the MCD+HC and HF+HC diet-fed groups showed higher TLR4 protein expression than those from the other corresponding groups (Supporting Fig. 7C,F). No significant difference was observed in the mRNA expression levels of TLR4 among the corresponding groups (Supporting Fig. 7C,F).

HSC Activation in NASH Down-Regulates PPARγ Expression and Enhances Both SREBP2 and miR-33a Signaling; Increased Cholesterol Intake Intensifies These Effects. As noted in the whole livers, the mRNA expression levels of collagen 1α1, collagen 1α2, and α smooth muscle actin (αSMA) were significantly increased in HSCs from the MCD and HF diet-fed groups compared with the corresponding control diet-fed groups. These increases were significantly enhanced by the increased intake of cholesterol (Fig. 1A,D).

The mRNA expression levels of PPARγ1 in HSCs were significantly lower in the MCD and HF diet-fed groups than in the corresponding control diet-fed groups. In addition, these decreases were significantly

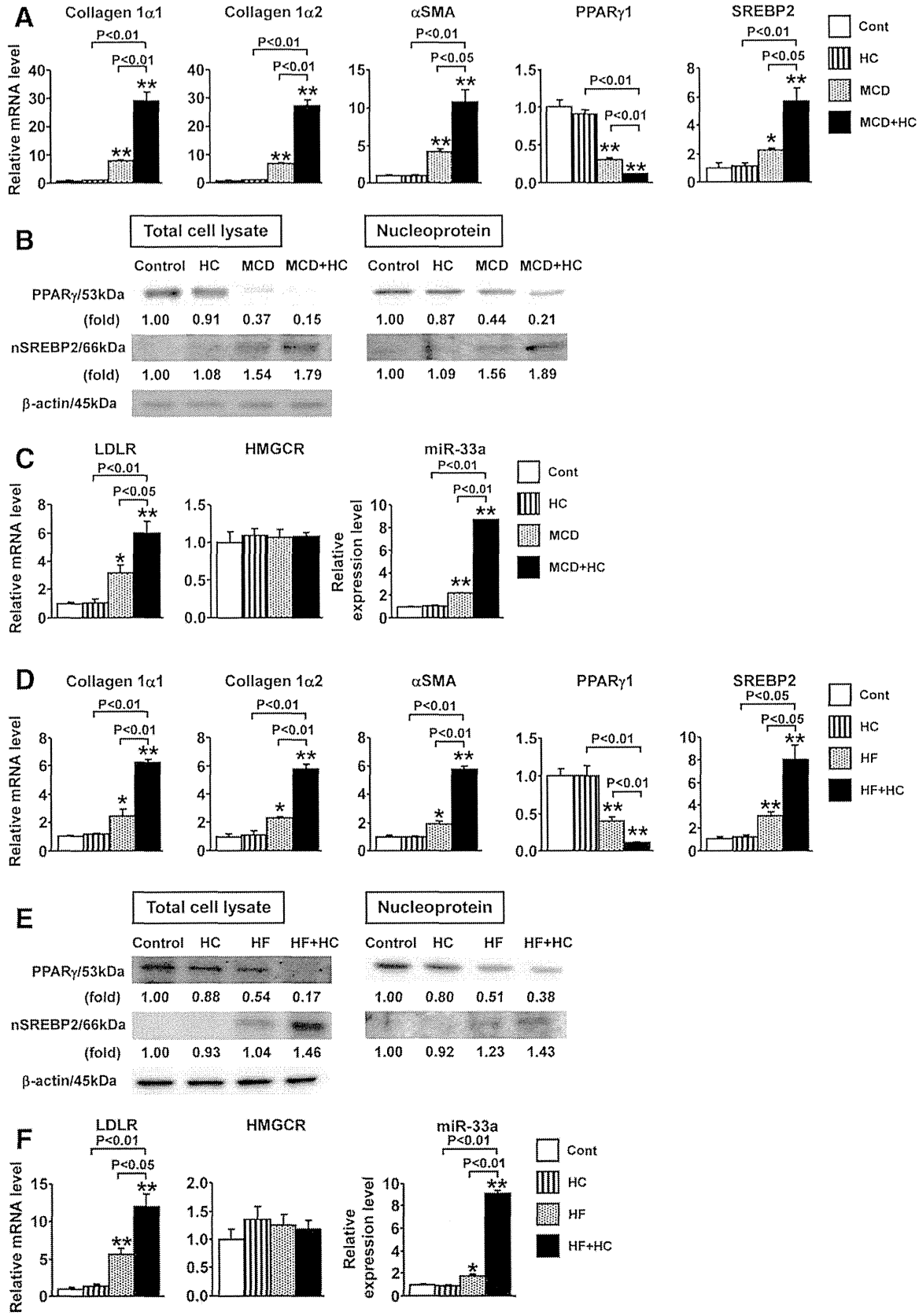

Fig. 1. Down-regulated PPARγ expression and enhanced SREBP2 and miR-33a signaling after HSC activation in the two mouse models of NASH. C57BL/6 mice (9 weeks old, male; n = 6-9/group) were fed (A-C) the control, HC, MCD, or MCD+HC diet for 12 weeks or (D-F) the control, HC, HF, or HF+HC diet for 24 weeks. (A,D) Quantification of collagen 1α1, collagen 1α2, αSMA, PPARγ1, and SREBP2 mRNA in HSCs isolated from the mice in each group. $^{**}P < 0.01$ and $^{*}P < 0.05$, compared with the control diet group. (B,E) Total and nuclear expression of PPARγ and SREBP2 protein in HSCs isolated from the mice in each group. The relative protein levels are indicated below the corresponding bands. (C,F) Quantification of LDLR and HMGCR mRNA, and miR-33a in HSCs isolated from the mice in each group. $^{**}P < 0.01$ and $^{*}P < 0.05$, compared with the control diet group. All data are expressed as means (SEM).

enhanced by the increased intake of cholesterol (Fig. 1A,D). Contrarily, the mRNA expression levels of SREBP2 were significantly higher in HSCs from the MCD and HF diet-fed groups than in those from the corresponding control diet-fed groups, and these increases were significantly enhanced by the increased intake of cholesterol (Fig. 1A,D).

The total and nuclear protein levels of PPARγ were lower in HSCs from the MCD and HF diet-fed groups than in those from the corresponding control diet-fed groups and these decreases were significantly enhanced by the increased intake of cholesterol (Fig. 1B,E). Meanwhile, the levels of the nuclear form of SREBP2 were significantly higher in HSCs from the MCD and HF diet-fed groups than in those from the corresponding control diet-fed groups. Furthermore, these increases were significantly enhanced by the increased intake of cholesterol (Fig. 1B,E).

Similar to SREBP2 expression, the expression levels of LDLR and miR-33a in HSCs were significantly higher in the MCD and HF diet-fed groups than in the corresponding control diet-fed groups. These increases were significantly enhanced by the increased intake of cholesterol (Fig. 1C,F).

In Vitro *HSC Activation Down-Regulates PPARγ Signaling, Which Enhances SREBP2 and miR-33a Signaling.* The total and nuclear forms of PPARγ were abundant in day 1 (quiescent) HSCs but declined in day 3 and 5 (activating) and day 7 (activated) HSCs (Fig. 2A). Meanwhile, the nuclear form of SREBP2 was scarce in day 1 HSCs, and its expression increased at days 3 and 5, and day 7 HSCs (Fig. 2A). Correspondingly, the PPARγ1 and SREBP2 mRNA expression levels were similar to the protein expression levels (Fig. 2A). Furthermore, the expression levels of LDLR and miR-33a in HSCs increased along with their activation (Fig. 2B).

PPARγ-siRNA treatment significantly increased the expression levels of SREBP2, LDLR, and miR-33a in quiescent HSCs (Fig. 2C). Similarly, treatment with the PPARγ antagonist significantly increased the expression levels of SREBP2, LDLR, and miR-33a in quiescent HSCs in a dose-dependent manner (Fig. 2D). On the other hand, overexpression (O/E) of PPARγ1 significantly decreased the levels of SREBP2, LDLR, and miR-33a expression in activated HSCs (Fig. 2E).

SREBP2-siRNA treatment significantly decreased the mRNA expression level of LDLR (Fig. 2F). The addition of PPARγ-siRNA did not affect the mRNA expression level of LDLR in quiescent HSCs treated with SREBP2-siRNA (Fig. 2F).

Enhancement of LDLR Expression and miR-33a Signaling Plays a Role in FC Accumulation in HSCs, Which Subsequently Increases TLR4 Protein Expression Through Suppression of the Endosomal-Lysosomal Degradation Pathway of TLR4. Suppression of LDLR mRNA expression by LDLR-siRNA treatment significantly decreased FC accumulation in HSCs treated with LDL or FBS (Fig. 3A). In HSCs treated with LDL or FBS, FC accumulation significantly decreased with the addition of anti-miR33a and increased with the addition of pre-miR33a (Fig. 3B). Furthermore, FC accumulation in HSCs increased along with their activation (Fig. 3C).

TLR4 protein expression, but not mRNA expression, in HSCs increased along with their activation (Fig. 3D). Treatment with LDL significantly increased TLR4 protein expression in HSCs and suppression of LDLR expression significantly decreased it (Fig. 3E). Similarly, the LDL-induced increase in TLR4 protein expression was significantly suppressed by the addition of anti-miR33a and significantly enhanced by the addition of pre-miR33a (Fig. 3E).

Furthermore, treatment with LDL significantly suppressed the ligand-mediated enhanced degradation of TLR4 in HSCs (Fig. 4A). Both chloroquine, an inhibitor of the endosomal-lysosomal pathways, and MG-132, an inhibitor of the proteosomal pathways, significantly increased TLR4 protein expression in HSCs (Fig. 4B). The addition of LDL did not affect the protein expression levels of TLR4 in HSCs treated with chloroquine, whereas it significantly increased the protein levels of TLR4 in HSCs treated with MG-132 (Fig. 4C,D).

FC Accumulation in HSCs Sensitizes These Cells to TGFβ-Induced Activation Through Enhancement of TLR4-Mediated Down-Regulation of Bambi. The mRNA level of Bambi significantly decreased with LPS treatment, and furthermore, the addition of LDL significantly enhanced the decrease in wild-type HSCs (Fig. 5B). A deficiency in TLR4 signaling reversed these decreases (Fig. 5B).

Wild-type HSCs, pretreated with LPS, demonstrated significant enhancement of collagen 1α1 and 1α2 mRNA expressions when stimulated with TGFβ, and showed a further increase in mRNA expression of collagen 1α1 and 1α2 when treated with LDL (Fig. 5C). A deficiency in TLR4 signaling, however, eliminated these increases (Fig. 5C).

Bambi mRNA expression did not decrease in HSCs treated with LDL, LDLR-siRNA, anti-miR33a, or pre-miR33a in the absence of LPS, but it significantly decreased when HSCs were treated with LPS

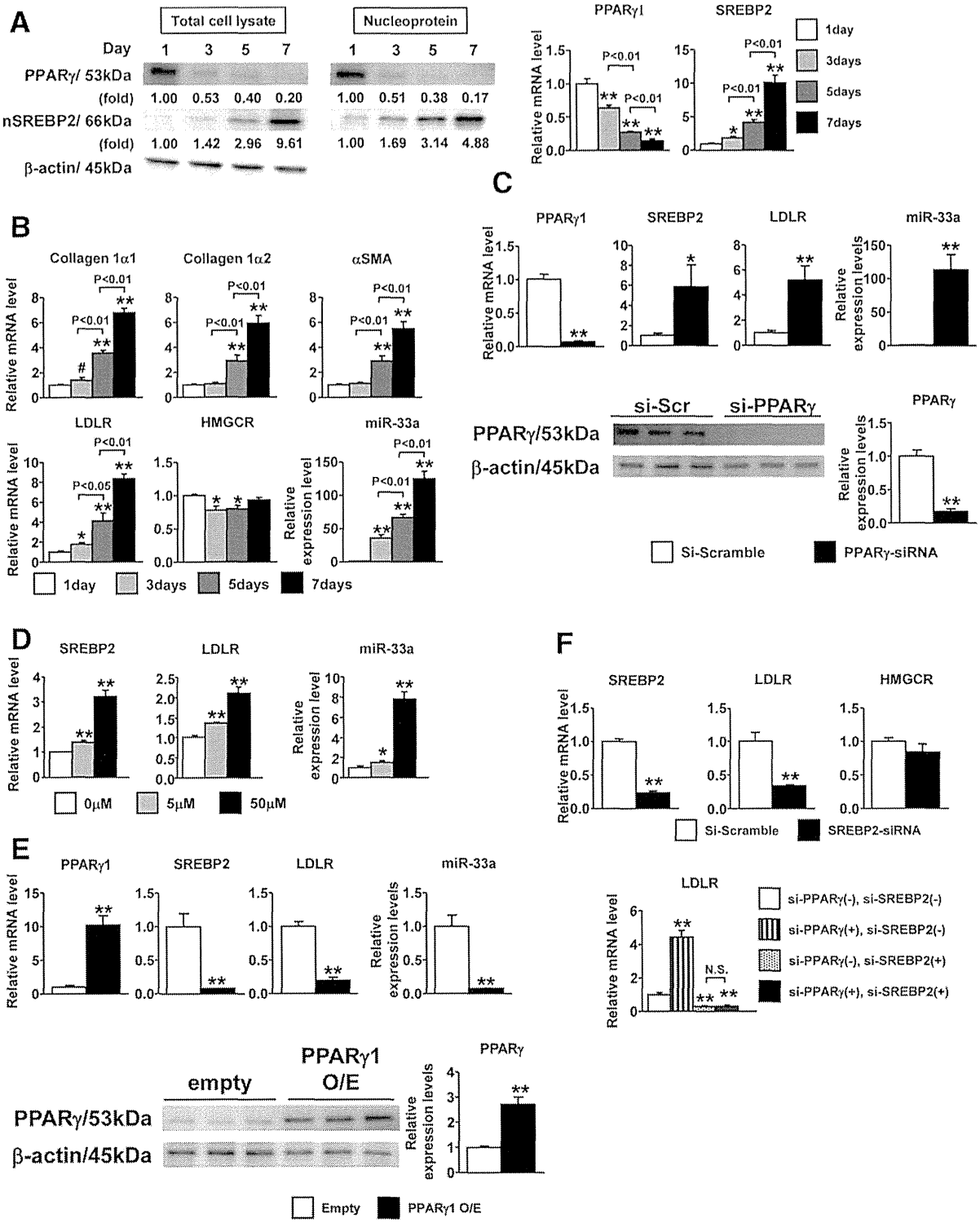

Fig. 2. Down-regulated PPARγ expression and enhanced SREBP2 and miR-33a signaling after HSC activation *in vitro*. (A) Total and nuclear protein expression (left panel) and mRNA levels (right panel) of PPARγ and SREBP2 in HSCs cultured for 1, 3, 5, or 7 days after isolation from C57BL/6 mice. The relative protein levels are indicated below the corresponding bands. $^{**}P < 0.01$, compared with the day 1 culture. (B) Quantification of collagen 1α1, collagen 1α2, αSMA, LDLR, and HMGCR mRNA and miR-33a in HSCs cultured for 1, 3, 5, or 7 days after isolation from C57BL/6 mice. Reflecting the activation of HSCs, the mRNA expression levels of collagen 1α1, collagen 1α2, and αSMA gradually increased from day 1 HSCs to day 3 and 5 HSCs to day 7 HSCs. $^{**}P < 0.01$ and $^{*}P < 0.05$, compared with the day 1 cultures. (C) Quantification of PPARγ1, SREBP2, and LDLR mRNA and miR-33a (upper panel) and PPARγ protein (lower panel) in quiescent HSCs treated with PPARγ-siRNA. $^{**}P < 0.01$ and $^{*}P < 0.05$, compared with the control culture. (D) Quantification of SREBP2 and LDLR mRNA and miR-33a in quiescent HSCs treated with the PPARγ antagonist at the indicated concentrations. $^{**}P < 0.01$ and $^{*}P < 0.05$, compared with the control culture. (E) Quantification of PPARγ1, SREBP2, and LDLR mRNA and miR-33a (upper panel), and PPARγ protein (lower panel) in activated HSCs treated with PPARγ1-O/E vector. $^{**}P < 0.01$, compared with the control culture. (F) Quantification of SREBP2, LDLR, and HMGCR mRNA in activated HSCs treated with SREBP2-siRNA (upper panel). Quantification of LDLR mRNA in quiescent HSCs treated with PPARγ-siRNA and/or SREBP2-siRNA (lower panel). $^{**}P < 0.01$, compared with the control culture. All data are expressed as means (SEM).

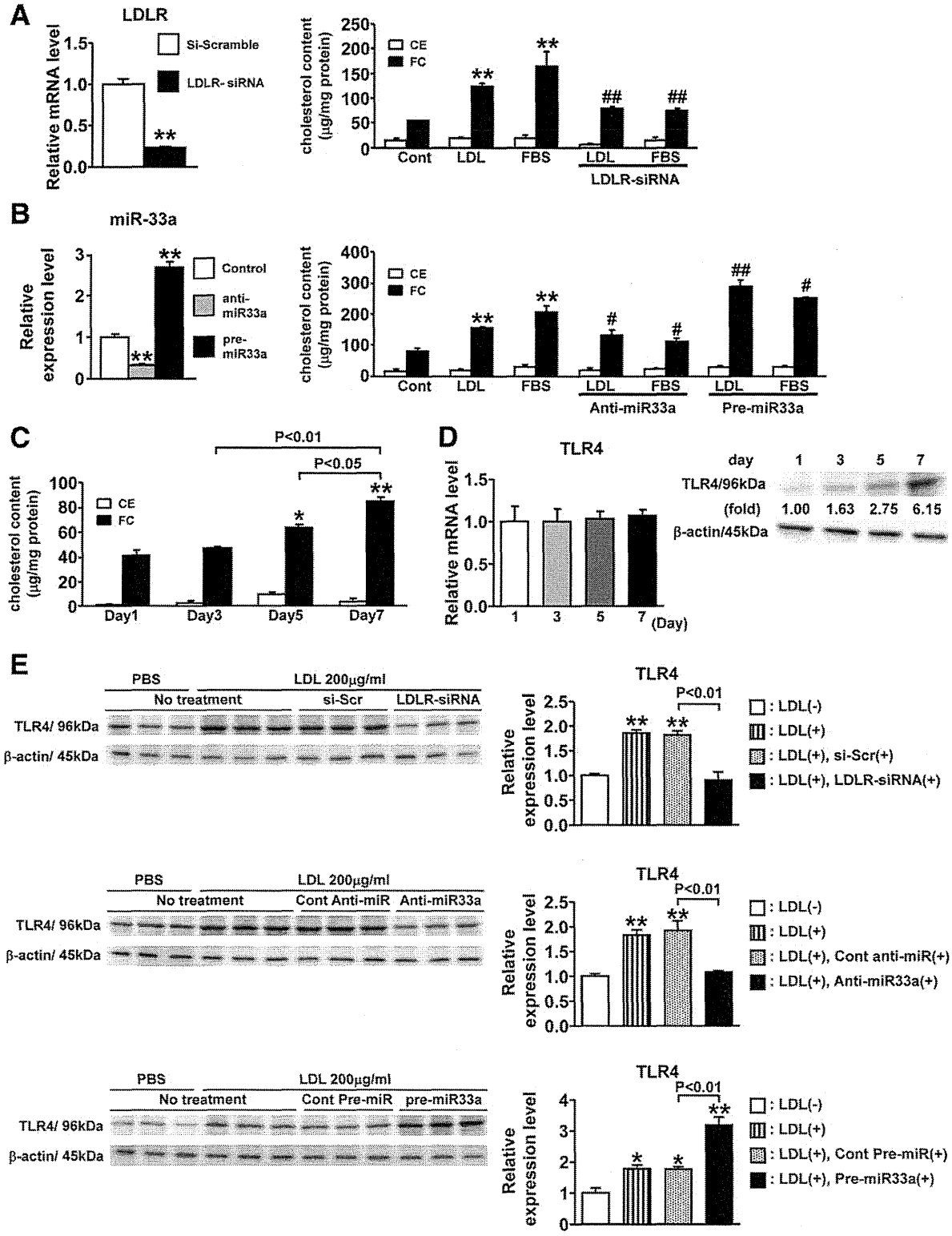

Fig. 3. FC accumulation in HSCs due to enhanced LDLR expression and miR-33a signaling. (A) Quantification of LDLR mRNA (left panel) and cellular FC and CE (right panel) in HSCs treated with LDLR-siRNA in the presence of LDL or FBS. (B) Quantification of miR-33a (left panel) and cellular FC and CE (right panel) in HSCs treated with anti-miR33a or pre-miR33a in the presence of LDL or FBS. $^{**}P < 0.01$, compared with the control culture. $^{\#\#}P < 0.01$ and $^{\#}P < 0.05$, compared with the FC contents in the corresponding cultures without the addition of LDLR-siRNA, anti-miR33a, or pre-miR33a. (C) Quantification of cellular FC and CE in HSCs cultured for 1, 3, 5, or 7 days after isolation from C57BL/6 mice. $^{**}P < 0.01$ and $^{*}P < 0.05$, compared with the day 1 cultures. (D) Quantification of TLR4 mRNA (left panel) and expression of TLR4 protein (right panel) in HSCs cultured for 1, 3, 5, or 7 days after isolation from C57BL/6 mice. The relative protein levels are indicated below the corresponding bands. (E) Expression (left panels) and quantification (right panels) of TLR4 protein in HSCs treated with control-siRNA, LDLR-siRNA, anti-miR33a, pre-miR33a, or control-miR33a in the presence of LDL. $^{**}P < 0.01$ and $^{*}P < 0.05$, compared with the control culture. All data are expressed as means (SEM).

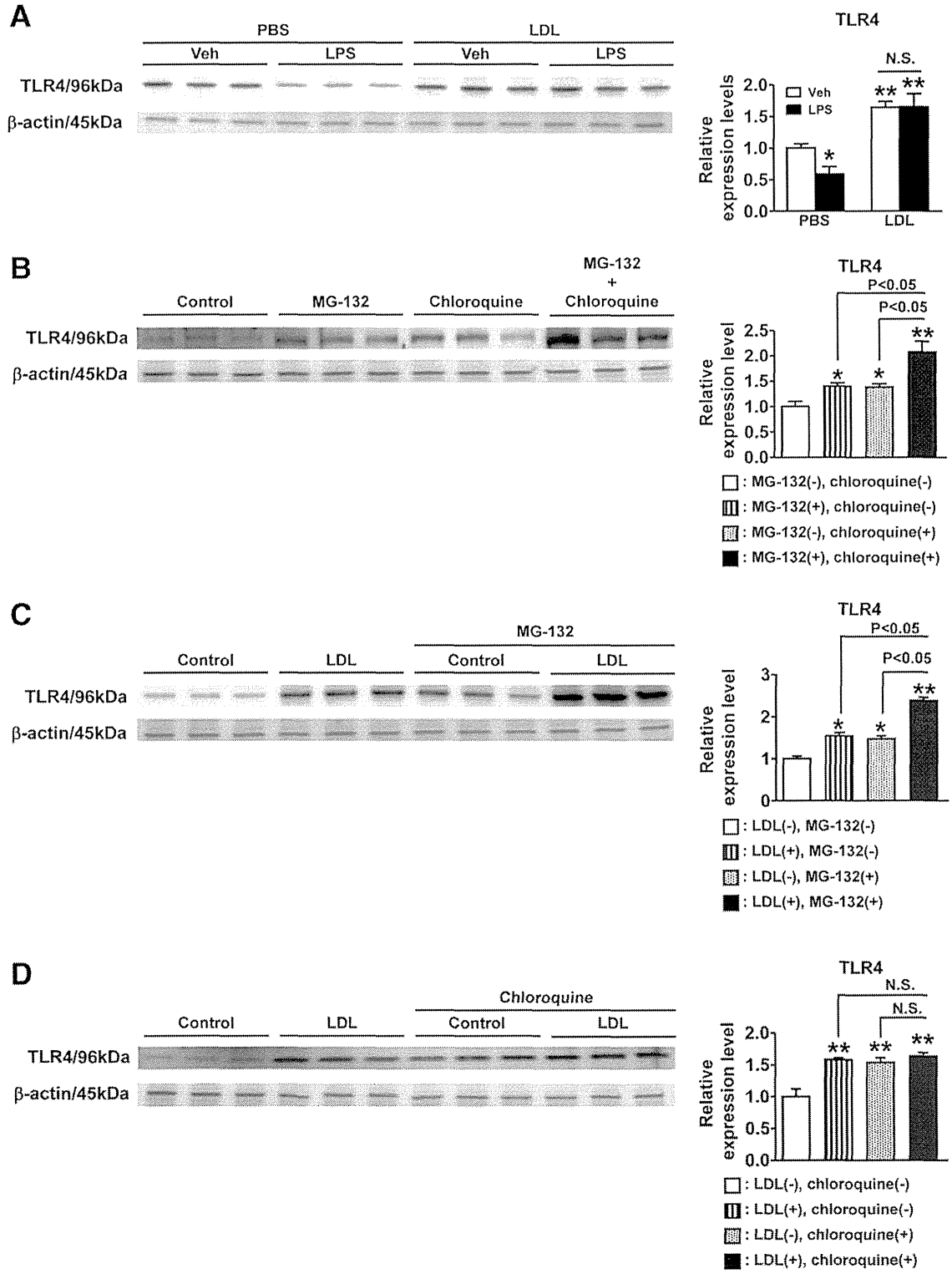

Fig. 4. FC accumulation in HSCs enhances TLR4 protein expression by suppressing the endosomal-lysosomal degradation pathway of TLR4. (A) Expression and quantification of TLR4 protein expression in vehicle-treated or LDL-treated HSCs, 60 minutes after addition of LPS (100 ng/mL), compared with cells not treated with LPS. $^{**}P < 0.01$ and $^{*}P < 0.05$, compared with the control culture, without LPS treatment. (B) Expression and quantification of TLR4 protein expression in HSCs treated with MG-132 and/or chloroquine. $^{**}P < 0.01$ and $^{*}P < 0.05$, compared with the control culture. (C) Expression and quantification of TLR4 protein expression in HSCs treated with LDL in the presence/absence of MG-132. $^{**}P < 0.01$ and $^{*}P < 0.05$, compared with the control culture. (D) Expression and quantification of TLR4 protein expression in HSCs treated with LDL in the presence/absence of chloroquine. $^{**}P < 0.01$, compared with the control culture. All data are expressed as means (SEM).

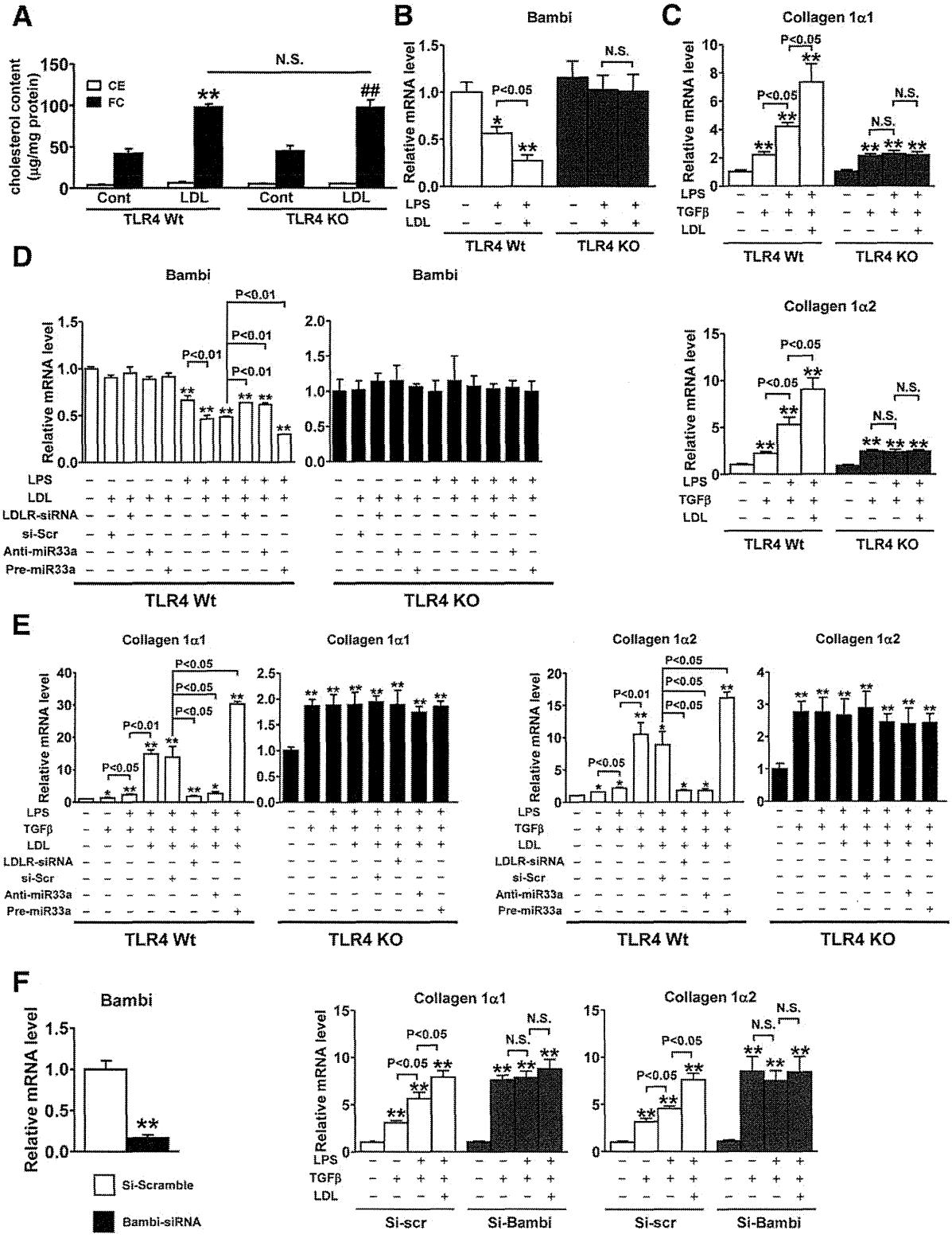

Fig. 5. FC accumulation in HSCs sensitizes HSCs to TGFβ-induced activation through enhancement of TLR4-mediated down-regulation of Bambi. (A) Quantification of cellular FC and CE in wild-type or TLR4-deficient HSCs, treated or untreated with LDL. $^{**}P < 0.01$ and $^{\#\#}P < 0.01$, compared with the corresponding control culture. (B) Quantification of Bambi mRNA in wild-type or TLR4-deficient HSCs, treated with LPS and/or LDL. $^{**}P < 0.01$ and $^{*}P < 0.05$, compared with the corresponding control culture. (C) Quantification of collagen 1α1 and collagen 1α2 mRNA in wild-type or TLR4-deficient HSCs, treated with LPS, TGFβ, and/or LDL. $^{**}P < 0.01$, compared with the corresponding control culture. (D) Quantification of Bambi mRNA in wild-type or TLR4-deficient HSCs, treated with LDLR-siRNA, control-siRNA, anti-miR33a, or pre-miR33a in the presence of LPS and/or LDL. $^{**}P < 0.01$, compared with the corresponding control culture. (E) Quantification of collagen 1α1 and collagen 1α2 mRNA in wild-type or TLR4-deficient HSCs, treated with LDLR-siRNA, control-siRNA, anti-miR33a, or pre-miR33a in the presence of LPS, TGFβ, and/or LDL. $^{**}P < 0.01$ and $^{*}P < 0.05$, compared with the corresponding control culture. (F) Quantification of Bambi mRNA in HSCs treated with Bambi-siRNA or control-siRNA (left panel). Quantification of collagen 1α1 and collagen 1α2 mRNA in wild-type HSCs, treated with Bambi-siRNA or control-siRNA in the presence of LPS, TGFβ, and/or LDL (right panel). $^{**}P < 0.01$, compared with the corresponding control culture. All data are expressed as means (SEM).

(Fig. 5D). This decrease was significantly enhanced in cells treated with LDL, whereas treatment with LDLR-siRNA reversed the LDL-induced decrease in Bambi mRNA expression (Fig. 5D). Similarly, treatment with anti-miR33a reversed the LDL-induced decrease in Bambi mRNA expression. On the other hand, treatment with pre-miR33a enhanced the LDL-induced decrease in Bambi mRNA expression (Fig. 5D). These results were in accordance with the results of FC accumulation and TLR4 protein expression in HSCs, and a deficiency in TLR4 signaling reversed all these changes (Fig. 5D).

Treatment with LDLR-siRNA reversed the LDL-induced increase in the mRNA expressions of collagen 1α1 and 1α2 in wild-type HSCs treated with LPS and TGFβ (Fig. 5E). In accordance with the results of FC accumulation and Bambi mRNA expression in HSCs, treatment with anti-miR33a reversed the LDL-induced increase in collagen 1α1 and 1α2 mRNA expression and treatment with pre-miR33a enhanced it (Fig. 5E). As is the case in Bambi mRNA expression, a deficiency in TLR4 signaling canceled all these LDL-induced changes in collagen 1α1 and 1α2 mRNA expression (Fig. 5E). In addition, treatment with Bambi-siRNA reversed the LDL-induced increase in the mRNA expression of collagen 1α1 and 1α2 in HSCs treated with LPS and TGFβ (Fig. 5F). Furthermore, in the same way as in the *in vitro* study, treatment with antagomirs against miR33a significantly alleviated the activation of HSCs in the mouse model of liver fibrosis induced by carbon tetrachloride (CCl_4). This occurred through the suppression of FC accumulation and the subsequent inhibition of TLR4-mediated down-regulation of Bambi in HSCs (Supporting Fig. 8).

Increased Intake of Cholesterol Does Not Impact Liver Fibrosis in NASH in TLR4-Deficient Mice. We used TLR4-deficient mice to assess whether the exacerbation of liver fibrosis in NASH by increased cholesterol intake was dependent on TLR4 signal transduction. Significant differences were not observed in the extent of liver fibrosis or in the hepatic mRNA levels of collagen 1α1, collagen 1α2, and αSMA, between MCD diet-fed and MCD+HC diet-fed TLR4-deficient mice (Fig. 6A-C). Similarly, the increased cholesterol intake did not enhance liver fibrosis in the HF diet-induced NASH in TLR4-deficient mice (Fig. 6D-F).

SREBP2-Mediated Feedback Regulation of Cholesterol Homeostasis Is Disrupted in HSCs and HSC Activation Further Enhances the Disruption. Nuclear accumulation of hepatic SREBP2 decreased in the two mouse models of NASH and further declined following supplementation with cholesterol (Supporting Fig. 9A). Cholesterol supplementation significantly decreased the hepatic mRNA levels of LDLR and HMGCR, which are downstream molecules of SREBP2, in both the animal models (Supporting Fig. 9B,C).

We next detailed the SREBP2-mediated feedback system of cholesterol homeostasis in hepatocytes and HSCs *in vitro*. The nuclear form of SREBP2 in hepatocytes was dramatically decreased by treatments with LDL (Fig. 7A) and 25-hydroxycholesterol, which promotes Scap-Insig complex formation.[11] These treatments also significantly decreased the nuclear form of SREBP2 in quiescent HSCs but did not affect that in activated HSCs (Fig. 7A). Quantitative analysis showed that the decrease was significantly enhanced in hepatocytes, compared with HSCs, and quiescent HSCs, compared with activated HSCs (Fig. 7A).

MβCD reportedly delivers cholesterol to cells without passing through lysosomes.[12] Treatment with a cholesterol-MβCD complex also dramatically decreased the nuclear form of SREBP2 in hepatocytes (Fig. 7A). This treatment significantly decreased the nuclear form of SREBP2 in quiescent HSCs but did not affect that in activated HSCs (Fig. 7A). Quantitative analysis showed that the decrease was significantly enhanced in hepatocytes, compared with HSCs, and in quiescent HSCs, compared with activated HSCs (Fig. 7A). Scap expression levels were much higher in quiescent and activated HSCs than in hepatocytes (Fig. 7B). However, the Insig-1 expression level in hepatocytes was comparable to that in quiescent HSCs; we did not detect any expression of Insig-1 in activated HSCs (Fig. 7B). Hepatocytes expressed Insig-2 protein, whereas we could not observe any expression of Insig-2 in HSCs (Fig. 7B).

A Scap trypsin cleavage assay[13] was subsequently performed to examine whether or not cholesterol-induced Scap conformational changes occurred in these cells. Scap, without cholesterol-induced conformational changes, yields a protected band of 27 kDa on sodium dodecyl sulfate-polyacrylamide gel electrophoresis (SDS-PAGE), whereas Scap, with the conformational change, yields a protected band of 26 kDa. Our data showed that the cholesterol-induced Scap conformational change in activated HSCs occurred to the same degree as that in quiescent HSCs or hepatocytes (Supporting Fig. 10A,B).

LDL treatment decreased the nuclear level of SREBP2 in quiescent HSCs. Treatment with Scap-siRNA or Insig-2-overexpression vector enhanced the effect, whereas treatment with Insig-1-siRNA

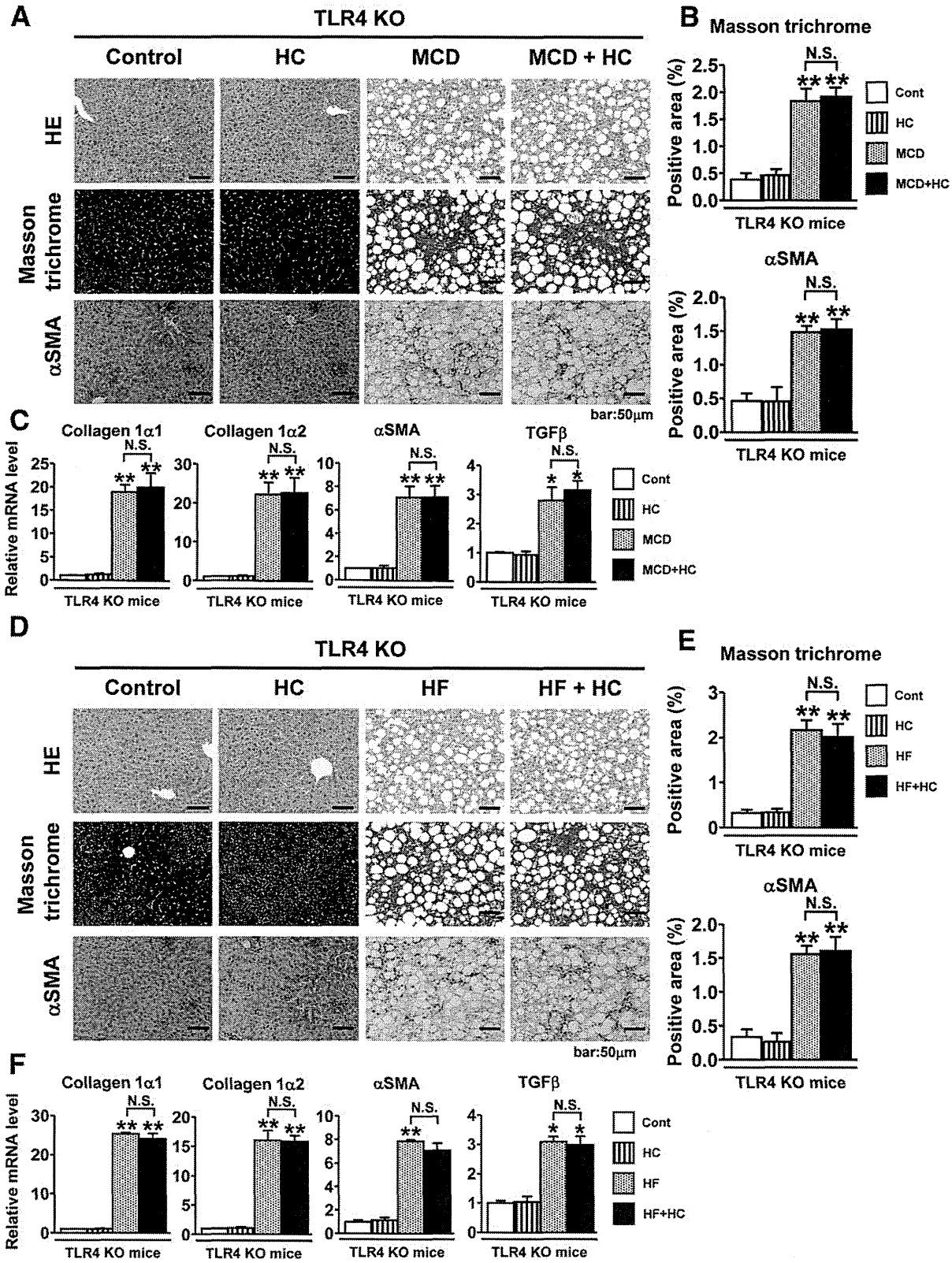

Fig. 6. Increased cholesterol intake does not impact liver fibrosis in NASH in TLR4-deficient mice. TLR4-deficient mice (7-8 weeks old; n = 4-7/group) were fed (A-C) the control, HC, MCD, or MCD+HC diet for 8 weeks or (D-F) the control, HC, HF, or HF+HC diet for 20 weeks. (A,D) Hematoxylin and eosin-stained, Masson's trichrome-stained, and αSMA-immunostained sections of representative liver samples. (B,E) Quantification of Masson's trichrome staining (upper panel) and αSMA immunostaining (lower panel). (C,F) Quantification of hepatic collagen 1α1, collagen 1α2, αSMA, and TGFβ mRNA. $^{**}P < 0.01$, compared with the control diet group. All data are expressed as means (SEM).

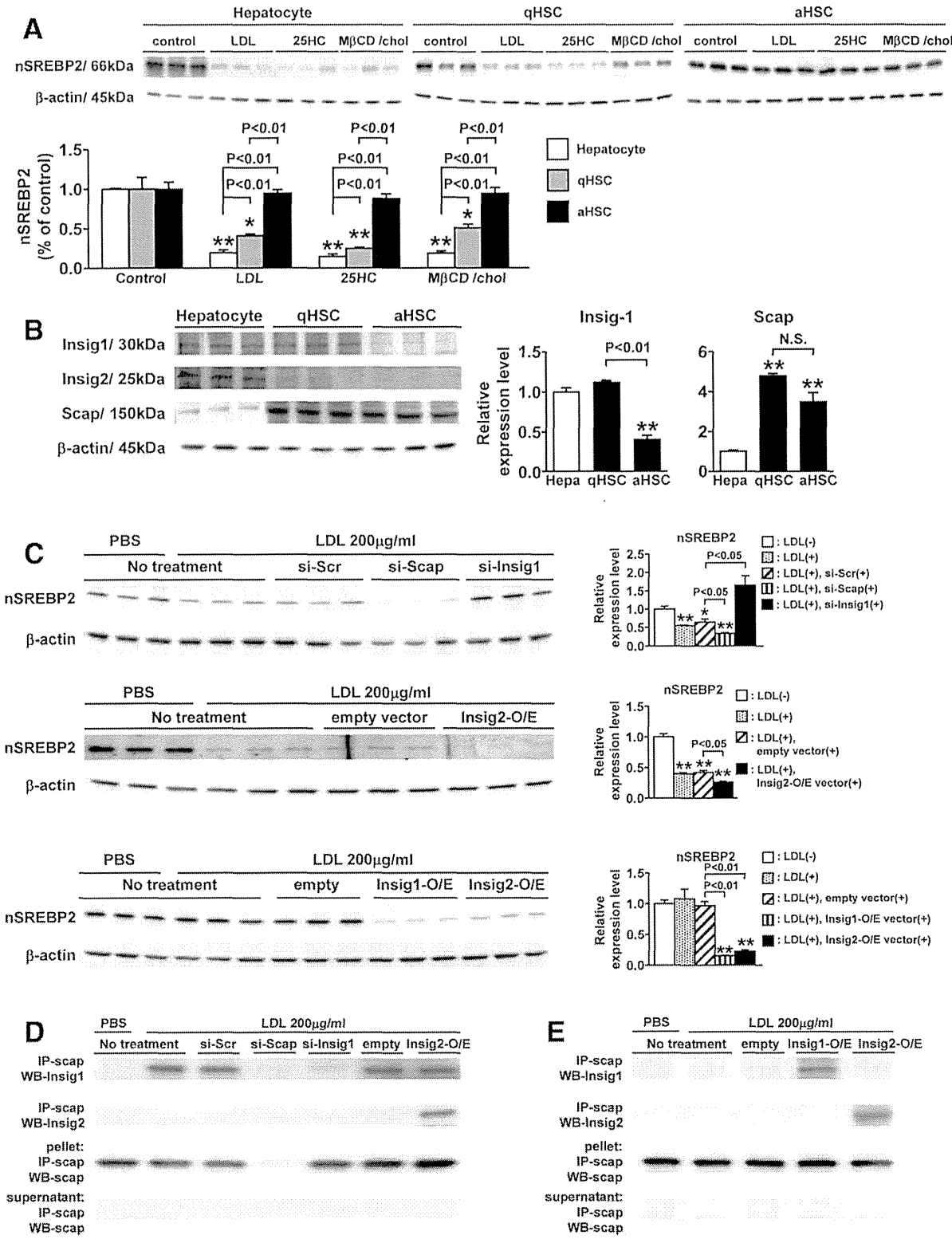

Fig. 7. The sterol regulatory systems in HSCs are disrupted and dependent on the relative amounts of Scap and Insigs. (A) Expression and quantification of the nuclear form of SREBP2 protein in hepatocytes, quiescent HSCs (qHSCs; cultured for 1 day after isolation), and activated HSCs (aHSCs; cultured for 7 days after isolation) after treatment with LDL, 25-hydroxycholesterol (25-HC), or MβCD/cholesterol complex. $^{**}P < 0.01$ and $^{*}P < 0.05$, compared with the corresponding control culture. (B) Expression and quantification of Insig-1, Insig-2, and Scap protein in hepatocytes, qHSCs, and aHSCs. $^{**}P < 0.01$, compared with the levels in hepatocytes. (C) Expression and quantification of the nuclear form of SREBP2 protein (upper panel) in qHSCs treated with Scap-siRNA, Insig-1-siRNA, or control-siRNA in the presence/absence of LDL, (middle panel) in qHSCs treated with Insig-2-O/E vector or control vector in the presence/absence of LDL, (lower panel) in aHSCs treated with Insig-1-O/E vector, Insig-2-O/E vector, or control vector in the presence/absence of LDL. $^{**}P < 0.01$ and $^{*}P < 0.05$, compared with the control culture. (D) Immunoprecipitation analysis of Scap-Insig-1 and Scap-Insig-2 complexes in qHSCs treated with control-siRNA, Scap-siRNA, Insig-1-siRNA, control vector, or Insig-2-O/E vector in the presence of LDL. (E) Immunoprecipitation analysis of Scap-Insig-1 and Scap-Insig-2 complexes in aHSCs treated with control vector, Insig-1-O/E vector, or Insig-2-O/E vector in the presence of LDL. All data are expressed as means (SEM).

counteracted the effect (Fig. 7C, upper and middle). However, LDL treatment did not affect the nuclear level of SREBP2 in activated HSCs; overexpression of Insig-1 or Insig-2 in HSCs significantly decreased the nuclear level of SREBP2 after the addition of LDL (Fig. 7C, lower).

LDL treatment increased the level of the Scap-Insig-1 complex in quiescent HSCs, whereas cotreatment with Scap-siRNA or Insig-1-siRNA reversed this change (Fig. 7D). We could not detect any Scap-Insig-2 complex in quiescent HSCs after the addition of LDL. Overexpression of Insig-2 increased the level of the Scap-Insig-2 complex in LDL-treated quiescent HSCs (Fig. 7D). On the other hand, neither the Scap-Insig-1 nor the Scap-Insig-2 complex could be detected in activated HSCs treated with LDL or not (Fig. 7E). Overexpression of Insig-1 increased the level of the Scap-Insig-1 complex in activated HSCs treated with LDL, and similarly, overexpression of Insig-2 increased the level of the Scap-Insig-2 complex after treatment with LDL (Fig. 7E).

In addition, the feedback regulation system of cholesterol homeostasis impacted the sensitization of HSCs to TGFβ-induced activation, in a manner similar to the FC accumulation system mediated by LDLR or miR33a (Supporting Fig. 11).

HSC Activation in NASH Down-Regulates Insig-1 Expression Through the Suppression of PPARγ Signal Transduction. The Insig-1 expression level was significantly lower in HSCs from the MCD and HF diet-fed groups than in those from the corresponding control diet-fed groups (Fig. 8A,B; Supporting Fig. 12A,B). These decreases were significantly enhanced by the increased intake of cholesterol (Fig. 8A,B; Supporting Fig. 12A,B). We could not detect any difference in the Scap expression level in HSCs among the groups (Fig. 8A,B; Supporting Fig. 12A,B).

Furthermore, Insig-1 protein was abundant in quiescent HSCs but its level declined at days 3 and 5, and day 7 HSCs (Supporting Fig. 12C). We could not detect any significant difference in the Scap expression level among the groups (Supporting Fig. 12C). Similar results were obtained in terms of the mRNA expression levels of Insig-1 and Scap (Supporting Fig. 12C). Treatment with the PPARγ antagonist significantly decreased the Insig-1 expression level in quiescent HSCs in a dose-dependent manner (Fig. 8C).

Discussion

This study showed that increased cholesterol intake accelerated liver fibrosis in the two mouse models of NASH without affecting the degree of hepatocellular injury or Kupffer cell activation. The exacerbation of liver fibrosis mainly involved FC accumulation in HSCs, which increased TLR4 protein levels through suppression of the endosomal-lysosomal degradation pathway of TLR4, down-regulated the expression of the TGFβ pseudoreceptor Bambi, and thereby sensitized the cells to TGFβ-induced activation. This study also showed that FC loading of HSCs is not sufficient to induce activation but serves to enhance activation initiated by TGFβ. These results are compatible with our previous finding[3] that showed that FC accumulation in HSCs increased membrane TLR4 levels; suppressed the HSC expression of Bambi, the TLR4 target gene[14]; and subsequently exaggerated liver fibrosis in mouse models of liver fibrosis.

This study also helped to elucidate the main mechanisms by which HSCs are sensitive to FC accumulation. The SREBP2-mediated feedback system, which plays a major role in maintaining cellular cholesterol homeostasis,[5,6] was disrupted in HSCs; this disruption could be attributed to high expression of Scap and no expression of Insig-2 in these cells. This could explain why the HC diet significantly reduced SREBP2 signaling in hepatocytes but not in HSCs, and resulted in enhanced FC accumulation in HSCs.

Furthermore, HSC activation sensitized these cells to FC accumulation. Repression of PPARγ signaling underlies HSC transdifferentiation.[15] In the present study, the level of PPARγ decreased along with the activation of HSCs. The suppression of PPARγ signaling in activated HSCs decreased the cellular expression of Insig-1, which resulted in enhancing the disruption of the SREBP2-mediated cholesterol-feedback system. This could partly explain why SREBP2 signaling in HSCs was enhanced, along with their activation, although FC accumulation continued to increase.

In addition, the decreased PPARγ signaling in activated HSCs also enhanced SREBP2 expression and signaling, resulting in enhanced expression of the LDLR, the SREBP2 target gene, in HSCs. As *SREBF2* is a bifunctional locus encoding SREBP2 and miR-33a,[10] suppression of PPARγ signaling also increased the level of miR-33a in HSCs, in turn suppressing the levels of NPC1 and ABCA1 (data not shown), which are negatively regulated by miR-33a.[10] These results showed that HSC activation enhanced FC accumulation, in part because of the increased LDLR level and the decreased NPC1 and ABCA1 levels.

The present results suggest that these characteristic mechanisms in HSCs could sensitize the cells to enhanced FC accumulation after increased intake of